Response to Reviewer #2 for Manuscript "High-Fidelity Modeling of Turbulent Mixing and Basal Melting in Seawater Intrusion Under Grounded Ice" by Mamer, Robel, Lai, Wilson, and Washam

Summary:
This paper studies the estuarine-type dynamics of seawater intrusion/subglacial discharge upstream of an ice sheet grounding line in a CFD model (ANSYS fluent). The subglacial environment is two-dimensional with a large aspect ratio (5cm high and 3-5m long) and is forced by fresh subglacial discharge upstream and salty inflow from the ocean downstream. The authors investigate the structure and distance of the saltwater intrusion, and its sensitivity to various parameters (primarily freshwater discharge velocity). They find that that the height of the subglacial environment and the velocity of the freshwater discharge are strong controls on the intrusion distance, and the strength of turbulent mixing has a somewhat weaker/more ambiguous effect. The authors also investigate basal melt at the upper surface of the subglacial region and how it affects the intrusion (to do so they must change the boundary condition at the top surface away from the no-slip condition), finding that melt decreases the intrusion distance, offering a possible negative feedback.
This is an interesting study of an important process; however, I have several major concerns with the paper that may affect the conclusions. If they are addressed, I would be happy to review a revised manuscript.

We appreciate the thoughtful review and valuable feedback given by reviewer 2. We have identified the reviewer's main concerns to be:

1. The lack of turbulence statistics in describing differences between laminar and turbulent cases and in justifying the modeling choices to vary C_μ.
2. The lack of a pressure and salinity dependent thermal boundary condition for the ice boundary. Furthermore, the lack of a free-slip case to compare with the melt-enabled simulations.
3. The incomplete discussion of a double-diffusive/diffusive mixing regime and inappropriate diffusive melting comparison to modeled melt.
4. Overall issues with clarity in describing the numerous simulations.

To address these concerns, we will re-run each of our simulations with a salinity and pressure-dependent thermal boundary condition and add additional cases with a free-slip ice kinematic boundary condition. In discussing model choices and comparing between cases of varying degrees of turbulent mixing, we will refer to model values of turbulent viscosity. The consideration of diffusive-convective mixing will be limited to the discussion section, and we will work to improve the clarity of the results and analysis.

Below, we address each concern in greater detail. The reviewer's comments are written in black, our responses are given in red, and the original manuscript text is in grey.

First Comment:

I am concerned about the turbulence modelling and the lack of inclusion of turbulence quantities in the paper. The fidelity (reported to be high!) of these simulations relies on the appropriateness of the turbulence closure, however, the reader is not given any context for the choice/s of C_mu,

We have added to line 563:

> "The typical value assigned to C_μ is 0.09, which has been empirically found for simple wall-bounded flows (Pope, 2000). However, for complex stratified flows or highly energetic jets, a standard constant value for the whole domain may not be appropriate (e.g. Lai et al. 2019). Based on equation 2, it is clear the value of C_μ is dependent on turbulence dynamics. However, in a modeling framework, we have to prescribe C_μ. Since a 'true' value for C_μ has not been found for the flow regime considered here (stratified and dynamically variable), we deemed it an appropriate approach to modulate this value to induce more or less turbulent mixing. In setting C_μ, we found numerical instability when $C_\mu \to 1$, therefore limiting our upper-end choice to a factor of 2 of the standard value used. For the lower-end case, we wanted to avoid choosing too low of a value, since the solution relaxes to laminar flow when $C_\mu \to 0$. This constrained our lower-end choice to a factor of 0.5 of the standard value."

Since C_μ away from the wall (near-wall would be set by the low-Reynolds formulation) can be found via the relationship:

$$C_\mu = \frac{\nu_t \epsilon}{k^2 \rho} \qquad \text{(R1)}$$

it is clear that the 'real' value of $C_\mu$is highly dependent on turbulence dynamics. In a modeling framework, we have to prescribe $C_\mu$to obtain eddy viscosity, it is not a post-processing derived value. Since a 'true' or 'real' value for $C_\mu$has not been found for the flow regime considered here (stratified), we deemed it an appropriate approach to modulate this value in order to induce more or less turbulent mixing. The goal in doing this is to answer a specific scientific question, namely: "What is the role of turbulent mixing in seawater intrusion and melting?"

The empirically derived value for C_μ that is traditionally used, 0.09, is for standard wall-bounded simple flow regimes. Under scenarios of high energetics (like a jet-plume) C_μ can approach 0.3 (Lai et al., 2019). For our fastest freshwater flux (Re = 2400), a jet-plume does form, therefore making a relatively increased C_μ value potentially realistic. Our original intention in setting C_μ was to span three orders of magnitude, with the standard value of 0.09 as the 'middle case'. However, initial runs demonstrated instability within the model

when C_μ was set to 0.9. On the other end, when C_μ is very low ($\rightarrow$ 0) the flow regime becomes laminar, which would not be helpful to address the research question at hand. Based on this, we chose to range the value by a factor of ¼ .

nor are we given any more intuitive quantities (e.g. the resulting turbulent diffusivity) to better understand the effect of varying C_mu, and how increased turbulence affects the flow.

We agree that turbulent viscosity would be more intuitive in explaining what changing the C_μ value results in. Here, we have plotted the turbulent viscosity (Figure R1) across all flux cases tested with each C_μ value in a simplified pipe flow example. For the revised simulations in our simulated domain, we will produce a similar figure that will be referenced in the appendix/supplementary.

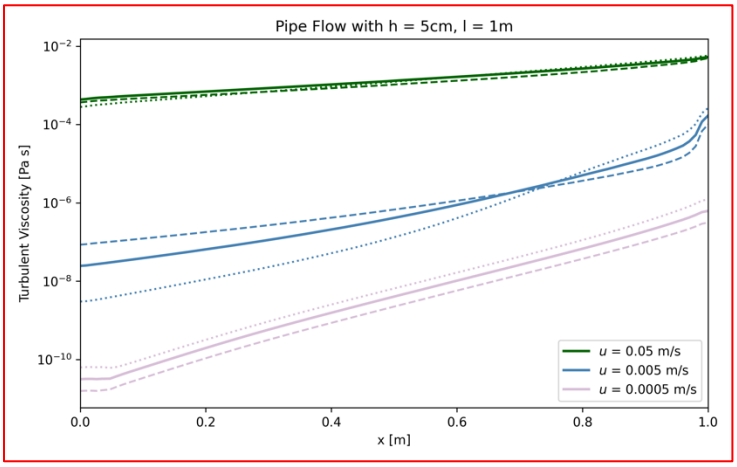

Figure R1

Turbulent Viscosity for each flux tested, with varied C_μ. Transects are taken along the middle of the pipe domain. The solid lines represent C_μ = 0.09, the dashed are for C_μ = 0.045, and the dotted lines are C_μ = 0.18. This is for a simplified pipe domain with length = 1m, height = 0.05m, and a velocity inlet prescribed at x = 1m. A pressure outlet (zero gradient flux boundary condition) is defined at x = 0m.

Without this information and context, I have low confidence in the modelling overall, especially since the effect of varying C_mu is non-monotonic for some cases (Fig 2B) and counter to my expectations for others (Figs 2A & C), i.e. I would have expected that increased mixing would decrease intrusion distance, whereas the authors find the opposite result.

Note, that the eddy viscosity in Figure R1 is lower than the molecular viscosity of water (~1.8e-3 Pa s) in most cases tested here, which indicates that turbulence does not play a dominant role in heat/salt/momentum transport. This likely contributes to our conclusion that turbulence in this domain does not affect intrusion distance significantly.

My recommendations to address this are as follows:

- Present the turbulent diffusivity (or viscosity) alongside T, S, u. In main MS or in a supplement

This will be done with the updated experiments, as demonstrated in Figure R1.

- Present the Reynolds numbers for the cases

This has been done. We have added to line 84:

> "The corresponding Reynolds numbers for the given geometry and freshwater flux are 25, 250, and 2500 for the low, medium, and fastest freshwater cases presented."

- Give some context for the choice of C_mu for similar flows – I presume the engineering literature can provide. Stratified plane couette flow may be a starting point in terms of a bounded, stratified flow.

We have modified line 563 as shown above.

Second Comment:

I don't understand why the temperature profiles have much sharper gradients than the salinity gradients (c.f. the darkest line in Fig A8A to the darkest line in Fig A8B). The authors mention the steep T gradients (not seen in S) in line 202 *(Such a steep thermocline is most likely due to the temperature boundary condition we imposed on the horizontal ice boundary)* however, I am concerned that the problem runs deeper than different boundary conditions. Why, for example, is temperature at 2cm depth at the GL entrance at 0.5 degrees (i.e. unmodified from ambient conditions), while salinity is <20ppt at the same location? There may be a serious issue with the mixing of these scalars which would significantly affect your results. Temperature-salinity plots may help determine if there is a problem.

We appreciate the reviewer bringing this to our attention. We have found a mis-assigned diffusion coefficient. We have re-run one non-melting scenario (u_f = 0.005 m/s, C_μ= 0.09) for the full model run-time (12 hrs at 5 s time steps). This updated diffusion coefficient does affect the horizontal gradient of salinity (Figure R2, panel B). Now, near the grounding line, both the temperature and salinity have been modified from ambient conditions. The quasi-steady-state intrusion distance is not greatly affected, with intrusion distance still at ~ 2m. In the updated model runs, we will use the correct haline diffusion coefficient.

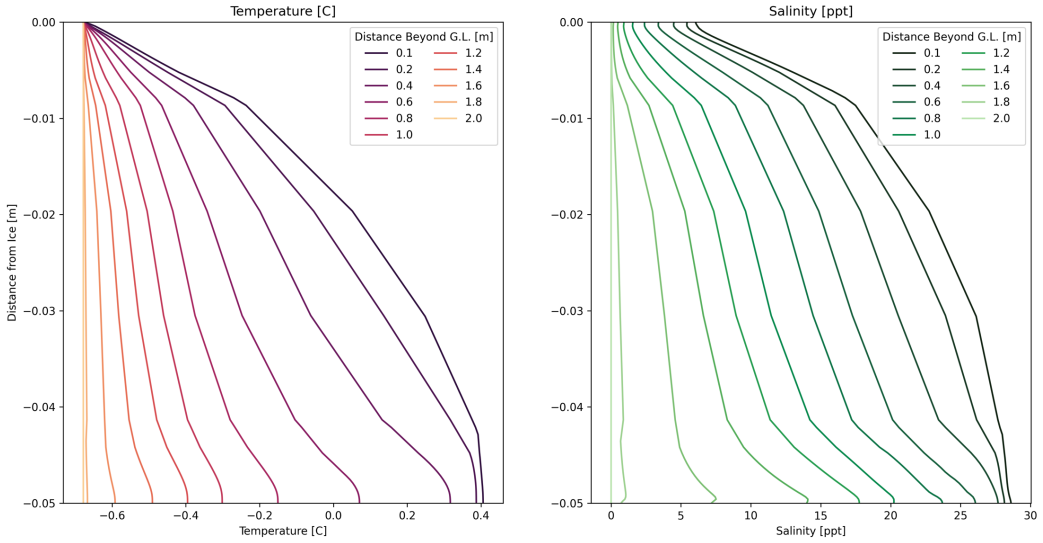

Figure R2

Vertical profiles of temperature and salinity at various distances upstream of the grounding line for experiments with fixed values for salinity fickian diffusion coefficient. These profiles are from the time-averaged simulation results, with a total model run time of 12 hrs at 5 s time steps. Ocean inlet conditions are 30 ppt and 0.5 deg C. Freshwater inlet conditions are set to the pressure freezing point at a glaciostatic pressure of 1000m and zero salinity. Note, that the freshwater temperature is negative because of new thermal boundary conditions that are dependent on pressure and salinity effects, further discussed in comment 6.

Third Comment

By comparing the temperature and salinity profiles as u_f is increased (Figs 3 A,B, Figs A8 A,B,D,E), it appears to me that the greatest control on mixing is time spent in the subglacial channel. For example, at u_f=0.05 cm/s salinity is quite well-mixed over the full depth of the channel, and varies mostly with distance along-channel, implying that diffusion (rather than advection) is dominating transport. For u_f=5cm/s, the top, outflowing layer remains fresh, indicating that the transport dominated by advection. This is somewhat counter to my expectations that turbulent mixing should be stronger for the higher velocity cases. This result should be investigated and discussed. As for comment (1), plots of the turbulent diffusivities for each case may be enlightening.

This is an interesting takeaway that we have not yet explored. We agree that this should be discussed and is potentially similar to observed characteristics in estuaries. In addition to the turbulent diffusivities, a local evaluation of the Peclet number may provide insight. It may also require investigating if this relationship is only dependent on freshwater velocity, or if the same vertical mixing characteristics develop for variable ocean velocity – even if intrusion distance does not change.

Added to line 207:

> "The degree of vertical mixing increases with decreasing freshwater velocity, which is similar to observed mixing dynamics in estuaries (Montagna 2012). For high freshwater fluxes, a well-developed salt-wedge forms and high stratification persists (Figure 3 panels A and B, Figure A8 panels A and B). For low freshwater fluxes, vertical mixing is strong and the water column homogenizes (Figure A8 panels D and E). Similar behavior is observed in estuaries, where estuaries dominated by tides and wind-driven mixing generate enough boundary shear to overcome stratification and initiate vertical mixing (Montagna 2012)."

Fourth Comment

The different BC between the melt-enabled and no-melt cases makes it impossible to attribute changes in the intrusion to the effect of melting alone. An additional case is needed with free slip and no melting to better separate these effects.

We agree that an additional free-slip case would benefit the analysis. As additional simulations, we will run each freshwater flux scenario with C_μ = 0.09 and a free-slip boundary. In Figure R3c below, we show an example of such flow for a simplified pipe flow case.

Fifth Comment

There are numerous different simulations included in the paper, however, few where one variable is systematically changed. This makes the paper/results hard to follow at times. A results table or bar chart showing how the intrusion distance changes across simulations would go some way to addressing this.

Based on this suggestion, we will revise the experiments table in the appendix (Table A2) and add it to the main body of the text. Referencing this table early on will help orient the experiments and results. We will include Reynolds number, intrusion distances, drag coefficients, statistics of melt rate, and statistics of mixing as well. It should then be clear that there is a "baseline case" and a number of experiments with only a parameter varied. However, there are other cases where we cannot avoid changing more than one model aspect at a time due to model limitations.

Sixth Comment

No salinity effect on the melt. In the simulations, the interface is salty (Fig 3E) which will act to depress the freezing temperature and therefore the interface temperature, altering the melt rate. The authors should state why they have not included this extremely

important effect (in more detail than “model limitations” line 437). In addition, some discussion of the likely effect of this simplification on the results is needed.

The thermal boundary condition for the ice boundary was originally chosen to keep the model simple. We expect that melt rates would only increase with a salinity and pressure-dependent boundary condition due to an increase in the overall thermal driving.

Based on recommendations from both reviewers, we will modify the thermal boundary condition of the upper boundary (‘the ice’) to be a function of near-ice salinity and a reference glaciostatic pressure (e.g. at 1000m).

We specifically edited lines 87 - 88:

> “The ice wall boundaries have a pressure and salinity-dependent thermal boundary condition of:
>
> $$T_b = S_b \lambda_1 + \lambda_2 + z \lambda_3 \quad \text{(R2)}$$
>
> Here, λ_1, λ_2, and λ_3 are constants, and the boundary salinity is S_b. The depth of the ice is equal to z_b, in these simulations we set this to be 1000 m. Both the vertical and horizontal ice boundaries have a no-slip kinematic condition in the non-melting cases, forcing the freestream fluid velocity to be zero at the ice wall.”

In addition, we have added to line 147:

> “Therefore, the melting cases have a free shear kinematic boundary condition. The temperature of the inflowing meltwater is set by equation R2.”

Where equation R2 is the pressure and salinity-dependent freezing point equation.

We have also edited lines 519 - 522 in the appendix:

> “For both melting and non-melting simulations, these ice walls have a thermal boundary condition dependent on near-wall salinity and pressure (eq. R2). Neither ice wall boundary allows for salinity diffusion, which would be another mechanism of melt to account for. The non-melting simulations employ a no-slip kinematic condition, which forces the fluid velocity to be zero at the wall. For melt-enabled cases, the top boundary of the subglacial space is turned into a velocity inlet to simulate melt. In designating this boundary as a velocity inlet, a free-slip kinematic condition is required. The downward vertical velocity set at the melting ice boundary follows equation 4. We turn off melting for the vertical ice boundary to

isolate the intrusion-induced melt from the vertical plume dynamics that would arise from the vertical ice boundary."

We will update the results and discussion section accordingly with the new simulations. Figure R3 is an example run of simplified pipe flow with such a thermal boundary condition.

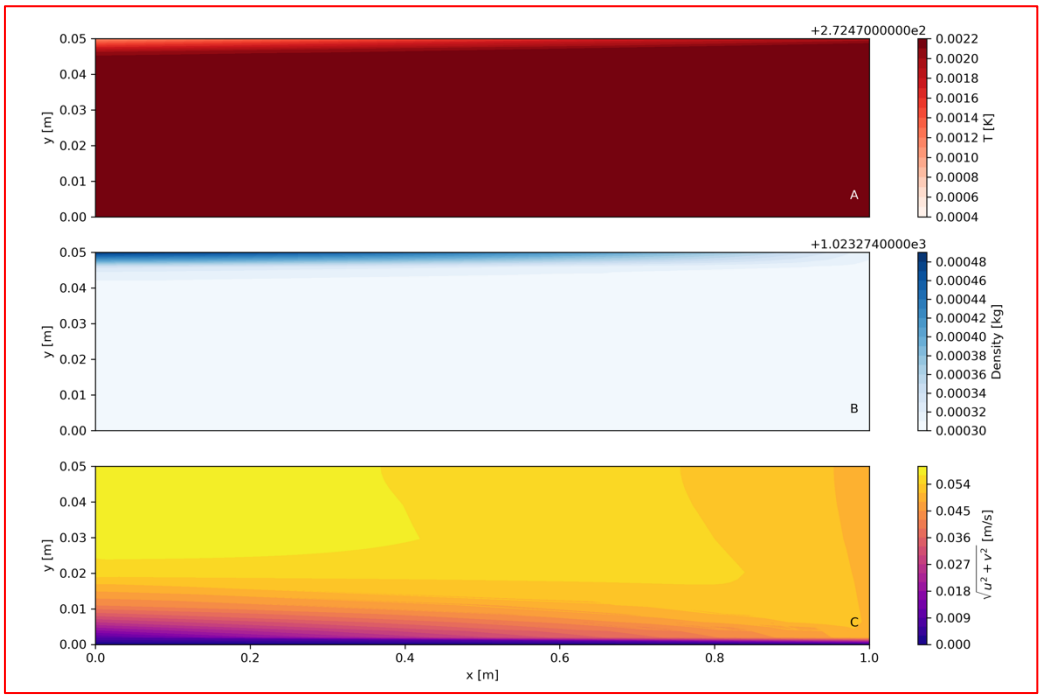

Figure R3

Example run of a 2D pipe-like geometry with ice at y = 0.05 m and a velocity inlet prescribed at x = 1m. A zero-gradient flux outlet is prescribed at x = 0 m. This case has a free-slip condition at the ice base (along y =0.05) as well as a salinity and pressure dependent thermal boundary condition (here, we set the ice thickness to be 1000 m). Panel A is temperature, panel B is density, and panel C is velocity magnitude. In panel C, a classical boundary layer forms along the flow direction at the bottom boundary where there is a no-slip condition. In panel A and B, a thin thermal boundary layer forms due to the salinity and pressure dependent thermal boundary condition cooling the near-ice water.

Seventh Comment

Double diffusive framework. Equation 9 is the same as Equation 4 (with marginally different thermal diffusivity) and is therefore not a parameterization to be tested, rather a re-stating of your melt BC. I propose removing Fig 6B and the "diffusive melt" in Fig 5. Notation m_DC and m_DDC (which are interchangeably used) are inappropriate here.

We recognize this and attempt to clarify that this comparison was not a parameterization to be tested, but rather a different 'transfer mechanism' (i.e. thermal diffusion instead of thermal conduction). However, we understand this may be redundant and not scientifically important and have removed it.

Eighth Comment

Transfer velocities/Stanton numbers (Figure 6)– I don't really understand the purpose of C and D. All D shows is the weak dependence of the Stanton number on ustar at low ustar (see the denominator of (7)), and all C shows is the same but multiplied by ustar. Since the S99 parameterization can't accurately predict melting for your simulations, this (trivial) result becomes misleading, as readers may think that it lends support to a certain Stanton number being useful more broadly for modelling ice-ocean interactions.

The intention of Figures 6C and 6D is to measure the turbulent transfer velocity (γ_T) and Stanton number using the physical flow-field values from our experiments. In doing so, we want to understand how 'efficient' this fluid domain is at transporting heat, relative to other published/observed values. Furthermore, we aim to explain how the value obtained for a Stanton number or turbulent transfer velocity is grid-dependent, meaning in a stratified regime with an interfacial shear layer you could have an order of magnitude difference depending on where the reference point is chosen. We recognize this result might be trivial, based on the turbulent transfer velocity's dependence on shear velocity. However, to think about parameterizing such a complex fluid regime, we may try to visualize how useful values (i.e. the Stanton number) vary vertically.

If you want to compare the Stanton number of your simulations to those found in the literature, you need to rearrange equation (6) less the conductive ice flux to solve for the Stanton number (and the (unitless) transfer coefficient \$Gamma_T$) using your model output melt rate, temperature etc.

We agree that there are benefits to both approaches and will also calculate this 'tuned' Stanton value with the new model results.

Other Comments

1. Line 83 – move references (carter…) after “non-summer months”
    - Fixed

2. Line 97 - “Our vertical domain size is at the upper bound of the viscous sublayer length scale that could exist between a well-mixed boundary layer and the ice” I don’t know what this means, please clarify.
    - The domain size and velocities (Reynolds number) used in these simulations constrain the development of the boundary layer and freestream flow. In this Reynolds number regime, we don’t see the development of a complete boundary layer with flow unaffected by the boundary (freestream flow)
    - To clarify, we have made these edits in the main text at lines 97 - 98:

      ~~“Our vertical domain size is at the upper bound of the viscous sublayer length scale that could exist between a well-mixed boundary layer and the ice (i.e. the vertical domain is small and does not include the turbulent outer layer).~~ For the tested freshwater velocities, the vertical domain size hinders the development of a full boundary layer. Instead, everywhere in the domain, the fluid feels the effects of the wall boundary.”

3. Line 154 – should be dT/dy in your coordinates
    - Fixed

4. Line 177 – “vary by a factor of 1000 **in response to the range of input velocities tested here**”.
    - Fixed

5. Line 179 – insert comma before “increased”
    - Fixed

6. Line 180 – “For the middle freshwater velocity (Figure 2 C),” - should this be 2A?
    - Fixed. We appreciate you finding this error.

7. Line 182 – “To contrast the effects of turbulent mixing, we tested a laminar flow case with no turbulent mixing (green line Figure 2 A) and saw no meaningful difference in intrusion distance.” It would be good to compare and contrast this case more, i.e. how different is the T/S structure? If it’s not different, then presumably turbulent mixing is not occurring in the channel.
    - We appreciate this suggestion and will include a more thorough exploration of the difference between turbulence viscosity, vertical structure (e.g. buoyancy frequency), and T/S space between the laminar and turbulent cases with the new simulation results.

8. Line 197/8 – refs should not be in parentheses.
    - Fixed.

9. Line 212 – How is Cd calculated? i.e. at what value of y are ustar and u evaluated? Also, as mentioned earlier I think Cd is a main result and this figure should come to the main text.

    - We will refine the drag figure in the appendix (Figure A5) and the methodology to calculate drag. We will add more discussion about our simulated drag coefficients to the results section with the new model results.

    - We have edited lines 140 - 141 in the main body:

        "Within the model framework here, the wall drag coefficient is not a free parameter to be set, but rather diagnosed from the simulations via the relationship (Pope, 2000):

        $$C_d = \frac{2\nu}{\overline{u^2}}\left(\frac{\partial \bar{u}}{\partial y}\right) \quad \text{(R3)}$$

        where $\partial\bar{u}/\partial y$ is the mean shear velocity and is evaluated over the upper 0.5 cm of the domain. The mean free stream current speed, $\bar{u}$, is obtained from the centerline flow. The kinematic viscosity is represented by ν. The full derivation of calculating the drag coefficient is given in section A4."

    We also added to section A4:

        "The drag coefficient cannot be prescribed for the simulations but is rather diagnosed from the model output. To do so, we use the relationship between the drag coefficient, C_d, and the wall shear stress, τ_w (Pope, 2000):

        $$C_d = 2\tau_w / (\rho\overline{u^2}) \quad \text{(R4)}$$

        The wall shear stress is equal to:

        $$\tau_w = \mu\left(\frac{\partial \bar{u}}{\partial y}\right) \quad \text{(R5)}$$

        and μ is the dynamic viscosity. We can rearrange and solve for C_d as a function of the near-wall velocity gradient as shown in equation R3."

10. Line 241 – “Reduction in velocity gradients arises from an increase in stratification, suppressing turbulence, and the kinematic boundary condition being a velocity inlet and not a no-slip wall.” – as per major comment 4, actually you can’t isolate these effects currently and a no-slip no-melt case is needed.
    - We appreciate this insight and agree with this recommendation. We will conduct a free-slip experiment to compare with the melt-enabled scenarios, per the suggestion in major comment 4. The comparison between melt-enabled cases and free-slip cases will replace lines 229-241.

11. Line 256 –Predominantly horizontal motion?
    - The motion is predominately horizontal from how the kinematic boundaries are prescribed. However, the horizontal density gradient that arises due to the characteristic ‘wedge’ shape of the seawater intrusion could introduce vertical convective motion to ‘flatten’ out the intrusion. This vertical motion may drive interfacial mixing and is an important mechanism to reduce the strength of stratification.
    - To further clarify, we have edited lines 252-258:

      “However, the horizontal density gradient introduced by the characteristic wedge shape of seawater intrusion will drive vertical baroclinic convective motion to flatten isopycnals. Such baroclinic adjustment may be an important source of interfacial mixing, working in tandem with turbulence and double-diffusive convection to reduce stratification within the subglacial environment. This convective-driven mixing mechanism differs from convective mixing caused by a sloping ice boundary, in which a buoyant plume may form. For the idealized scenarios in this study, buoyant convection via ice geometry will not drive mixing and thus melt since the ice is perfectly horizontal.”

12. Line 261 – again, you can’t attribute this to increased stratification (which MAY decrease shear/drag) because you haven’t isolated the effect of the no-slip BC (which WILL decrease shear/drag)
    - We appreciate this insight. Similar to comment 10, we will adjust any comparison in near-wall kinematics to be between a free-slip boundary and the melt-enabled cases.

13. Line 286 – Diffusive convective melting also involves convection driven by cooling and is different from diffusive melting. See Martin & Kauffman (1977) section 3 for diffusive melting and Martin & Kauffman (1977) section 4 for diffusive-convective melting.
    - We appreciate this insight. The results comparing melt rate parameterizations will be reworked in light of major comment 7. With this, we will clarify our intent to describe diffusive-convective melting and not diffusive melting.

14. Fig 3 – Is any averaging (time or space) done to obtain these profiles?
    - Yes, these are vertical profiles from the time-averaged domain. In order to clarify, we have edited the caption:

      > "Figure 3. Time-averaged vertical profiles of temperature(A, D), salinity(B, E), and x-component of velocity (C, F) along the seawater intrusion for uf =0.5 cm/s and medium turbulence Cμ = 0.09. The distance beyond the grounding line represents the distance (m) upstream of the fixed grounding line. The top row (A, B, C) is for the non-melt enabled case, i.e. the horizontal ice boundary is a wall boundary with a fixed temperature. The bottom row (D, E, F) is for the melt-enabled case where the ice boundary becomes a velocity inlet with freshwater inflow as a function of near-wall temperature."

      And figure discussion at line 200:

      > "The time-averaged vertical profiles of temperature, salinity, and velocity along the intrusion for non-melt-enabled cases (Figure 3) depict a two- layered flow in opposing directions, with a relatively uniform low-sloping vertical gradient in salinity, and a strong thermocline in the 2 cm directly below the ice."

15. Fig 3 - It would be great to see the systematic change in the intrusion as u_f is increased with a series of side-by-side plots, rather than having to move back and forward from figs 3 to A8.
    - We will take this into consideration and present the vertical profiles for the other freshwater velocity cases within the main text with results from the new simulations.

16. Line 319 – I would not say that the flow is weak at 5,10 cm/s. However, the height of the channel is very small, so the Reynolds number will be small. Again, Re or other turbulence metrics are needed.
    - All cases tested here have low Reynolds numbers ranging from 25 to 2500. We have added this to line 84:

      > "The corresponding Reynolds numbers for the given geometry and freshwater flux are 25, 250, and 2500 for the low, medium, and fastest freshwater cases presented."

    - In addition, the earlier suggestion to discuss turbulent viscosity metrics has been illuminating and we will use this variable to describe the energetics within the flow field for the new simulations.

17. Line 397 – how is the reduced gravity calculated here? Based on the density difference between the freshwater and saltwater?
    - The reduced gravity is calculated based on the density difference between pure freshwater and pure saltwater. However, a point can be made that the reduced gravity should change along the intrusion and amongst the freshwater cases based on the observation made in major comment 3. In the discussion, we will explore the sensitivity of the length scale proposed by Robel et al. 2022 to variations in reduced gravity.
    - To improve clarity, we have edited line 399:

      "Calculating the drag coefficient using model output gives Cd with values of order 10−2 to 100. The analytical theory of intrusion distance (L) for an unobstructed water sheet from Robel et al. (2022) is,

      $$L = \frac{H^2 g'}{4C_d^2 u_f^2}$$

      where H = 0.05 m is the height of the subglacial environment, g' = 0.20 m/s^2, and Cd is set to the maximum value within the intrusion. Reduced gravity is referenced to the density difference between the prescribed pure freshwater and pure seawater."

18. Line 427 – "If we anticipate viscous effects to dominate in seawater intrusions under grounded ice, then using the thermal and haline molecular diffusivities as so-called "transport velocities" would be appropriate, similar to the diffusive-convective framework presented above" – The units (m^2/s vs m/s) are not consistent. To turn the molecular diffusivity into a transport velocity, you need a lengthscale, i.e. the width of the diffusive sublayer. That's the hard part which is not addressed here!
    - We appreciate the reviewer's insight on this. With the model used here, we have a high enough domain resolution to identify the width of the diffusive sublayer. We can define this width to be where the turbulent viscosity is equal to the molecular viscosity. This works because the diffusive sublayer is where molecular diffusivity dominates. Therefore, there should be a point of transition where turbulent viscosity becomes weaker than molecular viscosity. This transition point (i.e. where they are equivalent) will represent the diffusive sublayer's thickness. We will present these results in tandem with the discussion of appropriate transfer mechanisms on line 427, highlighting the limitation of applying this method to large-scale coupled models.

    - We have edited line 427:

      "If we anticipate viscous effects to dominate in seawater intrusions under grounded ice, then using the thermal and haline molecular

diffusivities as so-called “transport velocities” would be appropriate. However, this would require knowing the width of the diffusive sublayer which, given computational constraints for coupled ice-ocean models, cannot be resolved.”

19. Figure 6 caption – The Stanton number should be γT /U, not γT /Cd
    - Fixed.

20. Figure 6 caption last line – are both the dashed and two solid lines from Washam et al 2023?
    - Both the dashed and solid lines are reported in Table 1 in Washam et al. 2023. However, the dashed line is reported first in Washam et al. (2020) and is cited as such in Table 1 of Washam et al. (2023).

21. Line 490 – “bolstering the idea that grounding zones are subglacial estuaries (Horgan et al., 2013).
    - No change is indicated in the comment.

22. Line 566 – seems like a note-to-self.
    - We appreciate you catching this. It has been removed.

23. Line 594 – either “given by (3)” or “given by equation 3”
    - Fixed.

24. The appendix is quite bloated. I think some of the figures could be relegated to SI and some should go to the main text. For example, I think Fig A5 is a key result and should go in the main text. Fig A1 could go in SI.
    - Based on recommendations from both reviewers, we will shorten the appendix to contain only descriptions of the model (equations, meshing, run-time settings). We will transfer the discussion of the drag coefficient to the main body under the results section. Sensitivity tests and model evaluation will go in Supplementary material.

25. Table A1 – inconsistent unit formatting (italics/roman). Look to TC style guide, or use roman which is typical. Units for theta should just be degrees.
    - We have made all units in Roman format and followed the TC style guide in handling denominator values.

26. Table A2 – again, unit formatting. H [cm]
    - We have made all the units in Roman format, following the TC style guide.

27. Figure A5 – the colours are too hard to tell apart.
    - We will refine this figure and include it in the main text.

28. Figures A9 & A10. The figures are labelled “law of the wall” but no interpretation is offered. What is the black vertical line and what does it mean? What would the profiles be expected to look like if a log layer was present? What portion of the flow is being shown? Is y+=0 at the top or bottom of the domain? Do we see a viscous boundary layer, i.e. u+=y+? in addition, it would be much more helpful if y+ was on the y axis, since that’s how the model is set up and how all your other profile plots are oriented.
    - We have combined A9 and A10 into one figure with the following caption: “Law of the wall for standard geometry cases with medium turbulence (C_μ = 0.09) for all velocities (Panels A-C). Law of the wall for the alternate geometry cases with medium turbulence(C_μ = 0.09) and freshwater velocity u_f = 0.5 cm/s (Panels C and D). In these figures, the vertical profiles are taken over the top half of the domain (2.5 cm from the ice face), to avoid effects from the intrusion interface. Therefore, y+ = 0 is at the top of the domain, where the ice boundary exists. The black line here represents y+ = 30, which would represent the point at which the log-law region of flow would develop and where u+ =y+. This point represents the transition to the fully turbulent outer boundary layer. Note how none of the profiles presented here cross that point, and therefore do not have a fully developed boundary layer.”

    - This figure will move to supplementary information and we will add a characteristic log law profile to demonstrate what the flow would look like for a fully developed boundary layer.

29. Reference 1 (Adusumilli) seems incomplete
    - Fixed.

Works Cited

Pope, S.B. (2000). Turbulent Flows. *Cambridge University Press*, Cambridge, 305-308.

Lai, C.C.K., Socolofsky, S.A. (2019). Budgets of turbulent kinetic energy, Reynolds stresses, and dissipation in a turbulent round jet discharged into a stagnant ambient. *Environ Fluid Mech* **19**, 349–377. https://doi.org/10.1007/s10652-018-9627-3

Montagna, P. A., Palmer, T. A., & Beseres Pollack, J. (2013). *Hydrological changes and estuarine dynamics* (1st ed. 2013.). Springer. https://doi.org/10.1007/978-1-4614-5833-3

Washam, P., Nicholls, K. W., Münchow, A., and Padman, L. (2020). Tidal Modulation of Buoyant Flow and Basal Melt Beneath Petermann Gletscher Ice Shelf, Greenland, J. Geophys. Res.-Oceans, 125, https://doi.org/10.1029/2020JC016427

Washam, P., Lawrence, J. D., Stevens, C. L., Hulbe, C. L., Horgan, H. J., Robinson, N. J., Stewart, C. L., Spears, A., Quartini, E., Hurwitz, B., Meister, M. R., Mullen, A. D., Dichek, D. J., Bryson, F., and Schmidt, B. E. (2023). Direct observations of melting, freezing, and ocean circulation in an ice shelf basal crevasse, Sci. Adv., 9, DOI:10.1126/sciadv.adi7638